Published in final edited form as:

Osteoarthritis Cartilage. 2025 July ; 33(7): 835–847. doi:10.1016/j.joca.2025.02.785.

Cartilage-targeting exosomes for delivery of receptor antagonist of interleukin-1 in osteoarthritis treatment

Tanvi Vinod Pathrikar[#], **Helna M. Baby**[#], **Bill Hakim**[#], **Hengli Zhang**[#], **Héctor A. Millán Cotto**[#], **Vineel Kondiboyina**[#], **Chenzhen Zhang**[#], **Ambika G. Bajpayee**[#,†,*]

[#] Department of Bioengineering, Northeastern University, Boston, MA 02115, USA

[†] Department of Chemical Engineering, Northeastern University, Boston, MA 02115, USA

SUMMARY

Objective: Exosomes are nano-sized cell-secreted vesicles naturally involved in joint tissue crosstalk and hold promise as drug carriers. Their negatively charged lipid bilayer, however, results in electrostatic repulsion from the anionic cartilage matrix limiting their applications in tissue targeting and drug delivery. Here we engineer cartilage targeting exosomes by reversing their net surface charge and use them for sustained delivery of interleukin-1 receptor antagonist (IL-1RA), a disease-modifying osteoarthritis (OA) drug that suffers from rapid joint clearance and poor cartilage uptake.

Design: Exosomes were surface modified by anchoring optimally charged cartilage targeting cationic motifs, Avidin (Av) and arginine-rich cationic peptide carrier (CPC). IL-1RA was surface anchored and encapsulated within the exosomes, creating two formulations: Exo_{Av}-IL-1RA and Exo_{CPC}-IL-1RA. Their penetration and retention in healthy and early OA cartilage were evaluated and compared with unmodified exosomes. The efficacy of Exo_{Av}-IL-1RA and Exo_{CPC}-IL-1RA in suppressing IL-1-induced tissue catabolism was tested using IL-1α challenged bovine cartilage explants over an 8-day culture period with a single dose and compared with free IL-1RA.

Results: Exo_{Av}-IL-1RA and Exo_{CPC}-IL-1RA, penetrated and retained in the full-thickness of early-stage arthritic cartilage explants. Free IL-1RA failed to suppress IL-1α-induced catabolism over the culture period. In contrast, Exo_{CPC}-IL-1RA significantly suppressed cytokine-induced glycosaminoglycan loss and nitrite release, enhancing cell metabolism and viability with only a one-time dose.

[*]Correspondence to: Departments of Bioengineering and Chemical Engineering, Northeastern University, Boston, MA, USA. a.bajpayee@northeastern.edu (A.G. Bajpayee).

Conflict of interest

The authors declare no conflict of interest.

Authors contribution

T.V.P. designed and implemented all the experiments and wrote the manuscript. H.M.B. contributed to the exosome harvest, surface modifications, biological experiments and writing the manuscript. B.H. supported the transport and microscale thermophoresis experiments. H.Z. supported the flow cytometry and transmission electron microscopy experiments. H.A.M. supported confocal imaging and microscale thermophoresis experiments. V.K. contributed to the design and implementation of the calcium signaling experiment and data analysis. C.Z. supported the exosome harvest and the surface modifications. A.G.B. conceived the idea, procured funding, designed experiments, oversaw data analysis and writing of the manuscript. All authors were involved in writing, reviewing, and approving the final version of the manuscript.

Conclusion: Cartilage targeting charge-reversed CPC anchored exosomes successfully targeted and delivered IL-1RA to early-stage arthritic cartilage. They hold promise as a cell-free intra-cartilage depot-forming carrier for sustained delivery of OA biologics.

Keywords

Exosomes; Osteoarthritis; Cartilage; Electrostatic Interactions; IL-1RA

Introduction

Exosomes are a diverse group of 30–200 nm-sized lipid bound particles that originate in the multivesicular bodies (MVBs) of their parent cells.[1] Exosomes are known to facilitate intercellular communication by transferring their cargo from the parent to recipient cells, thereby playing a role in biological crosstalk across multiple tissues and cells.[1,2] They have also garnered significant interest in drug delivery due to their high biocompatibility, cell-targeting properties and intrinsic therapeutic capabilities.[2,3] Multipotent progenitor mesenchymal stem cells (MSCs)-derived exosomes are emerging as promising therapeutics for osteoarthritis (OA) treatment.[4,5] These exosomes carry a wide range of regulatory microRNAs, messenger RNAs (mRNAs) and proteins (growth factors, cytokines, chemokines) that induce regenerative processes including chondrocyte migration, proliferation, differentiation, cartilage matrix synthesis and maintaining homeostasis.[4,6]

Cartilage is one of the primary tissues that is affected by OA. It is an avascular, aneural, and alymphatic tissue characterized by a complex extracellular matrix (ECM) composed of a dense network of collagen type II fibers and aggrecan glycosaminoglycans (GAGs), which contribute to a high negative fixed charge density (FCD) of −170 mM.[7] Direct intra-articular (IA) injections are used to deliver drugs to joint tissues, but both small and large molecules are rapidly cleared by subsynovial capillaries and lymphatics, respectively.[7] High negative FCD and the dense ECM of cartilage, along with rapid synovial clearance, make drug delivery to chondrocytes in deep cartilage layers extremely challenging. Cationic carriers that utilize electrostatic interactions have been shown to overcome these challenges by targeting the anionic tissue ECM and enhancing the rate of transport and intra-cartilage uptake of drug carriers through Donnan effects.[8–11] Although exosomes are naturally involved in joint tissue crosstalk and hold promise as drug carriers, their negatively charged lipid bilayer results in electrostatic repulsion from the anionic cartilage matrix. This limits their ability to effectively target cartilage for applications in drug delivery.[10,12] In our recent work, we addressed this challenge by reversing the net surface charge of exosomes through the anchoring of cartilage-targeting cationic motifs, enabling effective full-thickness penetration in early-stage arthritic cartilage and delivering loaded genes to chondrocytes while unmodified native exosomes failed to do so.[10]

Here, we engineer cartilage targeting exosome formulations for sustained delivery of larger-sized protein drugs. The receptor antagonist of interleukin-1 (IL-1RA) has been recognized as an effective disease-modifying osteoarthritic drug (DMOAD).[13] However, several preclinical studies and a few clinical trials testing IL-1RA as a therapeutic for OA have reported that the drug suffers from short joint residence, making it unable to provide

sustained benefit with a single dose.[14–19] The goal of this study is to enable sustained intra-cartilage delivery of IL-1RA using exosomes for cartilage repair. Our laboratory has designed an optimally charged, cartilage-targeting, depot-forming, arginine-rich hydrophilic cationic peptide carrier (CPC) with a net charge of +14 [RRRR(NNRRR)$_3$R].[20] CPCs exhibit 400 times higher intra-cartilage uptake compared to their uncharged equivalents, full-thickness penetration, and long-term retention in both healthy and arthritic cartilage tissue.[20] Avidin (Av), a cationic glycoprotein, has demonstrated similar intra-cartilage transport properties and has been utilized for the intra-cartilage delivery of OA drugs.[21] Both cationic carriers (Table I) leverage the high negative FCD of cartilage by using weak and reversible electrostatic interactions with the anionic GAGs to transport rapidly into the deep tissue layers in high concentrations due to Donnan effects.[9] In this study, two formulations Exo$_{Av}$-IL-1RA and Exo$_{CPC}$-IL-1RA are developed for sustained intra-cartilage depot delivery of IL-1RA (Fig. 1A). Despite the advantages of MSC-derived exosomes, the shortcomings such as complicated and expensive harvest procedures, low yields, and batch-to-batch variability, limits the clinical translation of exosome-based therapies.[22] Therefore, we use an alternative low-cost and high-yield source of bovine milk-derived exosomes in this work, especially because they have no immunological concerns.[23,24] The intra-cartilage depot-forming ability and biological activity of these formulations were evaluated in vitro using bovine cartilage explant OA models. Exo$_{CPC}$-IL-1RA was most effective in suppressing IL-1-induced catabolism in cartilage explants with only a one-time dose. This cartilage-targeting, charge-reversed exosome platform offers itself as a naturally derived cell-free carrier for the sustained delivery of OA drugs.

Materials and methods

Materials

The materials used for all the experimental procedures are described in Supplementary Information I.

Isolation of milk exosomes

Milk exosomes (Exos) were harvested according to our previously established protocol.[24] Briefly, diluted milk was treated with 0.25 M ethylenediaminetetraacetic acid (EDTA) on ice for 15 mins to chelate casein-calcium complexes and then subjected to differential ultracentrifugation. Finally, Exos were isolated using size exclusion chromatography (SEC) while protein content in individual fractions was determined via a bicinchoninic assay (BCA).

Synthesis of DSPE-PEG-IL-1RA

A lipid insertion approach was used to anchor IL-1RA onto Exos via maleimide-thiol conjugation of a DSPE-PEG (1,2-distearoyl-sn-glycero-3-phosphoethanolamine-N-[poly(ethylene glycol)-2000]) chain to the protein (Fig. 2A(iii)). To achieve this, 1 molar equivalent of DSPE-PEG-Maleimide (52 μg) in chloroform solution was added dropwise to 10 equivalents of unlabeled/fluorescein isothiocyanate (FITC)-labeled IL-1RA (30 μg) in 1X phosphate buffered saline (PBS) buffer (pH=7.0) while stirring continuously for 4 h at

room temperature. The product was then purified to remove the unreacted compounds using ultrafiltration and purified DSPE-PEG-IL-1RA was then stored at −20 °C until further use.

Encapsulation of IL-1RA in cationic exosomes

Sonication method was employed to encapsulate IL-1RA inside the cationic Exos based on a previous study with slight modifications.[25,26] 15 μg of unlabeled/FITC-labeled IL-1RA was added to the purified cationic exosomes and was sonicated for 12 s with 4 s pulse on and 2 s pulse off at 20% amplitude. The mixture was cooled on ice for 2 min and subjected to sonication again using QSonica Q125 Sonicator with a 1/8″ probe (Fisher Scientific) and unencapsulated IL-1RA was removed using ultrafiltration. Estimation of the encapsulation efficiency is described in Supplementary Information II.

Synthesis of IL-1RA-loaded cationic exosomes

To surface anchor IL-1RA on cationic Exos, two different methods were employed, (i) sequential and (ii) mixed pot reaction. For the sequential reaction, cationic Exos were synthesized first using Av and CPC, using our previously published protocol.[10,27] Following SEC purification, IL-1RA was encapsulated inside the Exos using sonication as described above. Finally, 21.5 μg (molar equivalent ratio, 1:1500, Exo: IL-1RA) of purified DSPE-PEG-IL-1RA was added dropwise to the cationic Exo solution. As a result, two cationic Exo formulations were synthesized: IL-1RA-loaded Exo_{Av} (Exo_{Av}-IL-1RA) and IL-1RA-loaded Exo_{CPC} (Exo_{CPC}-IL-1RA), which were used for further biological experiments.

Characterization of IL-1RA-loaded cationic exosomes

Size, zeta potential and polydispersity index (PDI) measurements, transmission electron microscopy (TEM) images, surface conjugation and IL-1RA loading confirmation images and flow cytometry were performed to characterize the cationic Exos. Additionally, the molecular interaction between Exos and DSPE-PEG lipid with Biotin/CPC/IL-1RA was measured by Microscale Thermophoresis (MST, NanoTemper Technologies) and the K_d (dissociation constant) values were estimated from the Hill equation.[24] In this assay, FITC-labeled Exo with constant concentration as the target, was titrated individually with serial dilutions of the ligands-unlabeled DSPE-PEG with Biotin/CPC/IL-1RA. Finally, the uptake, penetration and retention of IL-1RA loaded cationic exosomes was studied in healthy and early-stage arthritic bovine cartilage using the previously established protocols.[10,28] Details of the protocols are presented in Supplementary Information III.

Efficacy of IL-1RA-loaded cationic exosomes in bovine cartilage explants

3 mm (diameter) cartilage explants were harvested from 1–2-week-old young bovine femoral patellar grooves (Research 87, Boylston, MA) using dermal punches. Details of cartilage explant culture are provided in Supplementary Information IV.

Explants were pre-treated with IL-1α (2 ng/mL) for 48 h to generate initial GAG loss such that it can facilitate transport of 100–200 nm sized exosomes. 2 ng/mL IL-1α can create an early to mid-stage post-traumatic OA model in bovine cartilage explants by degrading the cartilage ECM, reducing chondrocyte viability and proteoglycan synthesis. The healthy control was supplemented with IL-1α-free media over 8 days. Previous work from our

lab shows that a one-dose administration of 5000 ng/mL of cationic IL-1RA-CPC+14 fusion protein suppressed IL-1α-induced catabolism over a period of 16 days by forming an intra-cartilage depot while a single equivalent dose of free IL-1RA failed to do so.[11] Hence, 5000 ng/mL of equivalent IL-1RA dose for all formulations was chosen as the testing concentration. To that end, explants were treated with single equivalent doses of (i) free unmodified IL-1RA, (ii) Exo_{Av}-IL-1RA, and (iii) Exo_{CPC}-IL-1RA after the IL-1α pretreatment to simulate one-time IA injection. Media supplemented with IL-1α was replenished every 48 h for 8 days.

At the end of the experiment, explants were digested with Proteinase K at 57 °C. To analyze the biological effects of cationic-motif-modified exosomes on the IL-1α induced degradation, the cumulative loss of GAGs in collected media samples and digested explants was measured using dimethyl-methylene blue assay.[8,11] Nitric oxide release was evaluated using Griess assay, along with cellular metabolism using Alamar blue assay.[13] Additionally, cartilage viability was assessed by staining full-thickness sections of explants with fluorescein diacetate and propidium iodide and imaged using a fluorescence microscope (ZEISS LSM 800).[8]

Calcium signaling

Effects of IL-1RA-loaded cationic exosomes on calcium signaling were studied using the previously established protocols[29] and is detailed in Supplementary Information V. Briefly, 3 mm x 1 mm bovine cartilage explants were harvested and treated with the same protocol as mentioned in above. On days 2 and 8, the explants were stained with calcium indicator dye (10 μM Calbryte 520 AM) and imaged over 10 mins using a confocal microscope (Zeiss LSM 800) to track the calcium signaling.

Statistical analysis

All biological explant studies used N = 6 explants for each condition with repeats from three independent animals as is consistent with previous research.[13] Animal was used as a random variable in a general linear effect model, and the data is shown as Mean ± Standard Deviation. Animal was found to have no effect, and thus, the data across animals is pooled. Tukey's Honestly Significant Difference test was utilized to compare different treatment conditions. P-values less than 0.05 were regarded as statistically significant. To avoid bias, biochemical experiments were carried out in duplicate, while image processing and analysis were done blindly.

Results

Harvest and surface modification of exosomes

The BCA assay revealed that fractions 5, 6, and 7 yielded the highest protein content (Fig. 3A), however, the nanoparticle tracking analysis (NTA) indicated that fractions 5 and 6 contained particles conforming to the size range of Exos and had a high concentration of particles (Fig. 3B). Therefore, fractions 5 and 6 were chosen from every harvest to obtain bovine milk-derived Exos. Applying the particle per protein ratio obtained using

Spectradyne nCS1 as detailed in our previous work,[24] Exos were aliquoted at 167 μg per tube.

Using the well-known Av-biotin noncovalent binding[30] and aqueous-based click chemistry, the surface of Exos was modified by conjugating Av and CPC, respectively, via sequential addition and mixed pot methods. The sequential addition approach was observed to be the most effective in reversing the charge of exosomes (Table II). This method yielded an optimized amount of IL-1RA loaded on the Exos compared to a mixed pot reaction (Supplementary Fig. 1). Additionally, using the sequential addition method, a molar equivalent ratio of 1: 2000: 2000 (Exo: Biotin: Av) resulted in a zeta potential of −2.3 ± 0.8 mV for Exo_{Av}-IL-1RA. Similarly, Exo_{CPC}-IL-1RA achieved a zeta potential of −1.6 ± 1.1 mV when used with a molar equivalent ratio of 1:8000 (Exo: CPC). This indicated that the surface charge of Exos was successfully reversed from −27.9 ± 3.0 mV to almost neutral zeta potential by anchoring the cationic motifs. Using fluorescently labeled CPC (Cy5) and Av (Texas Red), it was determined that one mole equivalent of Exo was surface anchored with 217 ± 33 mol equivalents of Av, and 1102 ± 29 mol equivalents of CPC. Loading of IL-1RA in Exos using probe sonication yielded 3.5 ± 0.8 μg in Exo_{Av} and Exo_{CPC} equivalent to 20 ± 3.2% encapsulation efficiency. Following sonication, IL-1RA-packed Exo_{Av} and Exo_{CPC} were incubated with DSPE-PEG-IL-1RA, which resulted in 4.2 ± 0.2 μg and 3.1 ± 0.3 μg of IL-1RA anchored on the surface of Exo_{Av} and Exo_{CPC} respectively. This resulted in a final loading of 7.6 ± 0.6 μg and 7.1 ± 0.8 μg IL-1RA loaded on Exo_{Av} and Exo_{CPC} respectively. These optimized formulations were used for all the subsequent experiments.

Characterization of IL-1RA-loaded cationic exosomes

Compared to native Exos, TEM images showed the identical size and consistent ‘saucer-like’ shape for surface-modified Exos, confirming that anchored motifs do not alter intrinsic morphology (Fig. 3C). The dark layers surrounding the modified Exos indicate successful conjugation of DSPE-PEG-CPC/Av/IL-1RA. To further confirm the conjugation of cationic motifs and IL-1RA on the Exos, CD63 coated magnetic beads anchored with dual-labeled and surface-modified Exos were imaged using a confocal microscope (Zeiss LSM 880) and analyzed using flow cytometry. For Exo_{Av}-IL-1RA, increased fluorescence of Texas Red and FITC from Av and IL-1RA, respectively, indicated successful loading on Exos (Fig. 3D (i)). Similarly, strong fluorescent signals of Cy5 and FITC from CPC and IL-1RA, respectively, were also an indication of effective loading on Exo_{CPC}-IL-1RA (Fig. 3D (ii)). To assess the strength of surface conjugation, binding affinities of DSPE-PEG-Biotin, DSPE-PEG-CPC, and DSPE-PEG-IL-1RA insertions in Exos were analyzed using MST. The K_d values revealed similar binding affinities as previously reported in the literature for lipid interactions.[24,31] All DSPE-PEG insertions in Exos yielded similar K_d values for lipid conjugates with Biotin, CPC, and IL-1RA, indicating that the addition of motifs to DSPE-PEG does not affect their binding affinity to Exos (Fig. 3E, Table III).

Enhanced transport of IL-1RA-loaded cationic exosomes in GAG-depleted bovine cartilage

To assess the transport and retention properties of IL-1RA-loaded native Exos, Exo_{Av}, and Exo_{CPC}, their one-dimensional transport from the superficial zone (SZ) to the deep zone

(DZ) was studied in healthy and trypsin-treated cartilage explants over a period of 24 h absorption followed by 24 h desorption in 1X PBS. In line with our earlier findings, Exo-IL-1RA, Exo_{Av}-IL-1RA, and Exo_{CPC}-IL-1RA were unable to penetrate through the healthy cartilage explants due to their large size compared to the pores in the ECM. Similarly, in trypsin-treated cartilage explants with 40% GAG depletion, electrically neutral Exo-IL-1RA did not penetrate the cartilage tissue (Fig. 4 (i)). Exo_{Av}-IL-1RA, however, penetrated into cartilage but failed to attain full-thickness penetration (Fig. 4 (ii)). Following 24 h desorption in 1X PBS, Exo_{Av}-IL-1RA was retained in the cartilage unlike Exo-IL-1RA (Fig. 4 (ii)). On the other hand, Exo_{CPC}-IL-1RA exhibited full thickness penetration in the GAG-depleted cartilage and was retained even after 24 h desorption in 1X PBS (Fig. 4 (iii)).

Single dose of IL-1RA-loaded cationic exosomes suppressed IL-1α induced catabolism

The therapeutic efficacy of a single dose of IL-1RA delivered using cationic Exos was evaluated in IL-1α induced arthritic bovine cartilage explants. IL-1α pretreatment for 2 days generated a GAG loss of 7.5 ± 1.1%. Consistent with the previous data, GAG loss increased significantly over 8 days in explants treated with IL-1α compared to the control group (Fig. 5B, red curve).[8,11,13] Additionally, a single dose of 5000 ng/mL free IL-1RA was unable to suppress the IL-1α-induced GAG loss over 8 days, which supports our previous findings (Fig. 5B, gray curve).[11] On the other hand, Exo_{Av}-IL-1RA and Exo_{CPC}-IL-1RA exhibited lower GAG release in the media after treatment on Day 0. However, Exo_{Av}-IL-1RA presented a suboptimal efficacy in reducing the IL-1α induced cartilage matrix degradation over a period of 8 days and resulted in cumulative GAG loss of 19.1 ± 2.6% by day 8 (Fig. 5B, yellow curve) ($p < 0.0001$). Of note, a single dose of Exo_{CPC}-IL-1RA resulted in significant suppression of cumulative GAG loss to 13.8 ± 1.4% (Fig. 5B, green curve) compared to the IL-1α group with a GAG loss of 23.4 ± 2.1% (Fig. 5B, red curve) ($p < 0.0001$). No significant difference was observed in the GAG loss levels between the control group (Fig. 5B, black curve) and Exo_{CPC}-IL-1RA over a period of 8 days ($p=0.72$). It should be noted that our previous work demonstrated that Exo_{Av} and Exo_{CPC} did not increase GAG loss compared to the control group, implying the biocompatibility of cationic Exo carriers.[10]

Cellular metabolism was assessed using Alamar blue assay 8 days after treatment in cartilage explants. A single dose of free IL-1RA ($p < 0.0001$) and Exo_{Av}-IL-1RA ($p < 0.0001$) was unable to restore the dysregulated chondrocyte metabolism induced by IL-1α treatment. In contrast, Exo_{CPC}-IL-1RA significantly rescued chondrocyte metabolism ($p=0.09$) and brought the levels back up to control levels (Fig. 5C). IL-1α mediated inflammatory reaction after treatment was evaluated by measuring nitrite release using Griess assay. Nitrite release was elevated in the IL-1α-treated group compared to the control group ($p < 0.0001$). A suppression in nitrite release levels was observed on day 2 in free IL-1RA ($p=0.002$), Exo_{Av}-IL-1RA ($p=0.002$) and Exo_{CPC}-IL-1RA ($p=0.03$) groups (Supplementary Fig. 2A) which was corroborated with the cartilage viability images (Supplementary Fig. 2B). However, with the introduction of Exo_{CPC}-IL-1RA, the nitrite release was significantly suppressed on day 8 compared to healthy control ($p=0.97$), indicating a modulated inflammatory response in the explants. Furthermore, the cartilage viability images on day 8 confirmed that a single dose of free IL-1RA and Exo_{Av}-IL-1RA

did not inhibit cell death stimulated by IL-1α. Conversely, Exo_{CPC}-IL-1RA exhibited enhanced cartilage viability after 8 days (Fig. 5D).

Calcium signaling

In chondrocytes, calcium signaling plays an important role as a secondary messenger that regulates cell metabolic processes.[32] Studies have shown that when joint physiology is altered, the reactions of chondrocytes to their peri-cellular surroundings are notably changed, potentially accelerating the onset or advancement of OA.[33,34] As a result, the calcium signaling characteristics are expected to alter significantly when treated with IL-1α.[34] Following the treatment regimen as mentioned in Efficacy of IL-1RA loaded cationic exosomes in bovine cartilage explants, calcium signaling was analyzed on days 2 and 8. The representative calcium oscillations on day 8 are shown in Fig. 6A and Supplementary Video 1–5. The representative calcium oscillations along with temporal parameters on day 2 are shown in Supplementary Fig. 3. Healthy control and Exo_{CPC}-IL-1RA demonstrated significantly higher response characteristics compared to the IL-1α control, IL-1RA and Exo_{Av}-IL-1RA (Fig. 6A). The temporal parameters of calcium signaling in the IL-1α differed significantly from the healthy control. On day 8, the duration of signaling (Fig. 6B) was longer in the IL-1α group (56.9 ± 12.9 s) ($p < 0.0001$), time between neighboring peaks (Fig. 6C) was lower (94.3 ± 19.8 s) ($p=0.048$) and the amplitude of signaling (Fig. 6D) (0.9 ± 0.3) ($p < 0.001$) also increased significantly compared to the healthy control group. These significant changes indicate the impact of IL-1α on the chondrocytes mimicking the effects of elevated cytokines in a post-traumatic osteoarthritis (PTOA) condition.[34] Similarly, the free IL-1RA group exhibited increased duration of signaling (56.1 ± 12.7 s) ($p < 0.0001$) and lower time between consecutive peaks (100.4 ± 15.7 s) ($p=0.02$) compared to the healthy control. However, IL-1RA group had elevated amplitude of signaling (0.7 ± 0.2) ($p=0.001$) potentially indicating chondrocyte death. In the Exo_{Av}-IL-1RA condition, no significant differences were observed in the duration of signaling (50.7 ± 8.4 s) ($p=0.55$) compared to the healthy control. Similar to IL-1RA, the amplitude (0.7 ± 0.2) ($p < 0.0001$) was elevated in Exo_{Av}-IL-1RA which may indicate chondrocyte apoptosis. Finally, for all three parameters, there was no significant difference between Exo_{CPC}-IL-1RA condition and healthy control group implying that Exo_{CPC}-IL-1RA is able to confer a protective effect against the impact of IL-1α.

Discussion

In this study, a novel cationic-motif-modified exosome platform was developed to enable intra-cartilage depot delivery of a disease-modifying OA drug, IL-1RA. The weak and reversible electrostatic binding interactions of these cationic-motif-modified exosomes with the negatively charged aggrecan GAGs facilitated improved targeting, penetration, and retention of IL-1RA within the cartilage tissue. Thus, a single dose of IL-1RA-loaded cationic-motif-modified exosomes significantly suppressed the catabolism induced in an early-stage arthritic model over a period of 8 days, while unmodified free IL-1RA did not.

Exosomes are naturally occurring extracellular vesicles that originate from the parent cells' MVBs.[35] The potential for surface modification further enhances the versatility of exosomes

as an effective delivery system.[36] Exosomes can be engineered to display specific surface ligands or cationic motifs, such as Av or CPC, chondrocyte affinity peptide, and fluorinated peptide dendrimers to improve targeting and binding to specific tissues.[10,27,37,38] Two formulations, Exo_{Av}-IL-1RA and Exo_{CPC}-IL-1RA, were designed by surface modifying exosomes with cartilage targeting cationic motifs, Av and CPC, while encapsulating IL-1RA inside the exosomes and also anchoring on their surface via sequential addition method. Both techniques, anchoring and encapsulation were employed for loading IL-1RA as both have their benefits and shortcomings. Anchoring on the surface ensures IL-1RA is readily available to interact with IL-1R1 receptor found on the surface of chondrocytes but risks degradation, while encapsulation protects IL-1RA but has to go through fusion with the plasma membrane of chondrocytes and endocytosis for the release.[3] Although this combination delivery of IL-1RA was effective in this work over 8 days, long-term potency of intra-cartilage exosome-mediated depot delivery of IL-1RA needs to be evaluated. Av glycoprotein was utilized here as it has been shown to effectively deliver small molecule OA drugs such as Dexamethasone and Kartogenin to cartilage cells and elicit prolonged therapeutic effects compared to free drugs by using electrostatic binding interactions with cartilage aggrecan-GAGs.[21,39,40] Similarly, cartilage-targeting arginine-rich CPC carrier was designed for carrying conjugated large protein drugs into deep cartilage layers rapidly in high concentrations. The presence of 14 arginine residues facilitates a high Donna partitioning of 3.4 at the cartilage-synovial fluid (SF) interface, enabling rapid, full-thickness penetration.[9,12,20] The hydrophilic asparagine spacers in the CPC minimize its competitive binding with hydrophobic SF constituents and enhance their cartilage targeting ability.[9] Using these cationic motif modifications, the net negative surface charge of exosomes was successfully reversed from −27 mV to −2.3 mV (Exo_{Av}-IL-1RA) and −1.6 mV (Exo_{CPC}-IL-1RA) (Table II). While the anchoring of Av and CPC on the surface of exosomes, did not fully reverse the overall macroscopic negative charge on the exosomes, on a microscale, a cationic delivery cascade was established that would result in the full thickness diffusion of the modified exosomes through an early-stage arthritic cartilage tissue.[10] Since zeta potential is the electrical potential measured at the slip plane, it does not correctly depict the net surface charge distribution.[41] Therefore, while the zeta potential represents a slightly negative charge, the microscale interactions of the cationic motifs with the negatively charged aggrecan GAGs facilitate the transport of modified exosomes into the cartilage tissue via weak reversible electrostatic interactions. Additionally, extensive work from our lab has established the safety of Av and CPC at high doses in cartilage.[21,42–44]

The cartilage transport and retention properties of the IL-1RA-loaded modified exosomes were evidently improved. Neither native exosomes nor IL-1RA-loaded modified exosomes were able to penetrate through healthy cartilage owing to the small pore size (~10 nm) of the cartilage ECM. Our recent work also corroborated these results, where the penetration of the native and modified exosomes was hindered in healthy cartilage tissue.[10] Additionally, Feng *et al.* have reported similar observations previously, where they found that the uptake and penetration of unmodified and surface-modified MSC-derived small extracellular vesicles was significantly hindered in normal pig cartilage tissue 24 h after the treatment.[45] However, Exo_{CPC}-IL-1RA demonstrated superior transport compared to both, Exo_{Av}-IL-1RA and native exosomes as it penetrated through the full thickness of the 40% GAG-depleted

cartilage tissue. In fact, the average gray value of the FITC fluorescence from IL-1RA on Exo_{CPC}-IL-1RA was 3.9 times higher than that of native exosomes and 1.5 times that of Exo_{Av}-IL-1RA (Supplementary Fig. 4). Additionally, Exo_{CPC}-IL-1RA was retained in 40% GAG-depleted cartilage 24 h after desorption in 1X PBS owing to the weak reversible electrostatic interactions (Fig. 4). Moreover, in our recent work, we have shown that a single dose of Exo-CPC successfully penetrated through the full thickness of Destabilized Medial Meniscus mouse knee cartilage 9 weeks post-surgery as well as early-stage arthritic human cartilage tissue in vitro.[10] However, long-term retention of these modified exosomes needs to be evaluated.

Post-injury induced OA patients are often rapid progressors due to the elevation of several pro-inflammatory cytokines.[46,47] During the early stages, although an initial loss of proteoglycans is observed, majority of GAGs are still preserved in the ECM.[48,49] At this stage, the ECM degradation is not severe enough to initiate collagen loss and hence the disease is in a reversible condition, allowing for the rescue of cartilage from further damage.[13,50] Early intervention at this critical juncture can be beneficial in slowing down the progression of OA, providing a window of opportunity to preserve joint function and minimize long-term damage. An early-stage arthritic condition was recapitulated in our in vitro efficacy studies with IL-1-induced catabolism to evaluate the potential of IL-1RA-loaded cationic-motif modified exosomes for early therapeutic interventions. In terms of therapeutic efficacy, a single dose of Exo_{CPC}-IL-1RA significantly suppressed GAG loss in IL-1α-induced arthritic cartilage explants over eight days. This was in stark contrast to free IL-1RA and Exo_{Av}-IL-1RA, which did not exhibit the same level of suppression of IL-1-induced catabolic activity. Moreover, the single-dose Exo_{CPC}-IL-1RA also rescued cellular metabolism and suppressed the nitrite release as well as restored cartilage viability (Fig. 5). Finally, calcium signaling is an important indicator of chondrocyte function and health. In this study, IL-1α disrupted calcium signaling, mimicking the effects of elevated inflammatory cytokines in PTOA conditions,[34] whereas the Exo_{CPC}-IL-1RA treated explants, demonstrated calcium signaling characteristics similar to the healthy control (Fig. 6). These results were corroborated with the cartilage viability images (Fig. 5). Overall, Exo_{CPC}-IL-1RA demonstrated superior cartilage penetration and effectively delivered IL-1RA to chondrocytes, resulting in significant therapeutic efficacy than Exo_{Av}-IL-1RA. The subpar efficacy of Exo_{Av}-IL-1RA can be attributed to the hindrance posed by the large size of surface functionalized globular Av protein (molecular weight [MW]~66 kDa), limiting the transport of exosomes within the cartilage matrix. Despite increased matrix pore size in 40% GAG-depleted cartilage explants and the positively charged surface of Exo_{Av}-IL-1RA, these modified exosomes were unable to penetrate through the full-thickness of cartilage, as evident from the 1D transport model (Fig. 4-ii). While Av functionalized exosomes did not perform as expected owing to their large size and aggregation issues,[10] CPC functionalization of exosomes helped create intra-cartilage drug depots to enable a sustained and targeted delivery of packed IL-1RA to chondrocytes residing in the deep cartilage layers. Therefore, cationic-motif-modified exosomes address the challenges associated with drug delivery for OA treatment due to high negative FCD of cartilage and rapid drug clearance from the joint space.

The intrinsic therapeutic potential of MSC-derived exosomes has been well-reported in numerous clinical trials. However, the clinical evidence supporting their use for OA is quite limited and can be attributed to compromised joint pharmacokinetics, low drug loading, and poor tissue targeting, which can be resolved through surface modification techniques. Nonetheless, several significant challenges need to be addressed for the clinical translation of surface-modified exosomes, including alterations in intrinsic bio-functionality after modification, long-term storage, and stability issues, and low yield following multiple purification processes.[35] Future research should focus on investigating the modification of MSC-derived exosomes with cationic motifs for dual treatment with loaded drugs or genes along with inherent therapeutic potential from the MSCs. Another future direction could be evaluating the long-term therapeutic effects and safety of Exo_{CPC}-IL-1RA in small animal models of OA to understand its potential for clinical application. This system could also be used for combinatorial therapy with different OA gene targets as it allows for drug or gene encapsulation as well as surface conjugation of drugs.[10] In conclusion, this study lays the groundwork for using engineered exosomes as a modular system for cartilage-targeted delivery of DMOADs.

Supplementary Material

Refer to Web version on PubMed Central for supplementary material.

Acknowledgments

We would like to thank the Amiji and Wanunu labs as well as the Institute for Chemical Imaging of Living Systems (CILS) at Northeastern University for their respective assistance with the ultracentrifuge, spectrophotometer and flow cytometry/imaging. We would also like to thank Dr. Ryan Porter at University of Arkansas for Medical Sciences for help with the nanoparticle tracking analysis data. Lastly, we would also like to thank all the members of the Molecular Bioelectrostatics and Drug Delivery lab at Northeastern University for the help and support.

Funding

Funded by the National Institute of Biomedical Imaging and Bioengineering (NIBIB) Trailblazer R21 (EB028385), NIH R01AR075121 and NSF CAREER Award 2141841.

References

1. Luan X, Sansanaphongpricha K, Myers I, Chen H, Yuan H, Sun D. Engineering exosomes as refined biological nanoplatforms for drug delivery. Acta Pharmacol Sin 2017;38:754–63. 10.1038/aps.2017.12 [PubMed: 28392567]
2. Herrmann IK, Wood MJA, Fuhrmann G. Extracellular vesicles as a next-generation drug delivery platform. Nat Nanotechnol 2021;16:748–59. 10.1038/s41565-021-00931-2 [PubMed: 34211166]
3. Zeng H, Guo S, Ren X, Wu Z, Liu S, Yao X. Current strategies for exosome cargo loading and targeting delivery. Cells 2023;12: 1416. 10.3390/cells12101416 [PubMed: 37408250]
4. Toh WS, Lai RC, Hui JHP, Lim SK. MSC exosome as a cell-free MSC therapy for cartilage regeneration: Implications for osteoarthritis treatment. Semin Cell Dev Biol 2017;67:56–64. 10.1016/j.semcdb.2016.11.008 [PubMed: 27871993]
5. De Bari C, Roelofs AJ. Stem cell-based therapeutic strategies for cartilage defects and osteoarthritis. Curr Opin Pharmacol 2018;40:74–80. 10.1016/j.coph.2018.03.009 [PubMed: 29625333]
6. Bao C, He C. The role and therapeutic potential of MSC-derived exosomes in osteoarthritis. Arch Biochem Biophys 2021;710, 109002. 10.1016/j.abb.2021.109002
7. Bajpayee AG, Grodzinsky AJ. Cartilage-targeting drug delivery: can electrostatic interactions help? Nat Rev Rheumatol 2017;13:183–93. 10.1038/nrrheum.2016.210 [PubMed: 28202920]

8. Vedadghavami A, Hakim B, He T, Bajpayee AG. Cationic peptide carriers enable long-term delivery of insulin-like growth factor-1 to suppress osteoarthritis-induced matrix degradation. Arthritis Res Ther 2022;24:172. 10.1186/s13075-022-02855-1 [PubMed: 35858920]
9. Vedadghavami A, He T, Zhang C, Amiji SM, Hakim B, Bajpayee AG. Charge-based drug delivery to cartilage: Hydrophobic and not electrostatic interactions are the dominant cause of competitive binding of cationic carriers in synovial fluid. Acta Biomater 2022;151:278–89. 10.1016/j.actbio.2022.08.010 [PubMed: 35963518]
10. Zhang C, Pathrikar TV, Baby HM, Li J, Zhang H, Selvadoss A, et al. Charge-reversed exosomes for targeted gene delivery to cartilage for osteoarthritis treatment. Small Methods 2024;8, e2301443. 10.1002/smtd.202301443
11. Mehta S, Boyer TL, Akhtar S, He T, Zhang C, Vedadghavami A, et al. Sustained intra-cartilage delivery of interleukin-1 receptor antagonist using cationic peptide and protein-based carriers. Osteoarthr Cartil 2023;31:780–92. 10.1016/j.joca.2023.01.573
12. Vedadghavami A, Zhang C, Bajpayee AG. Overcoming negatively charged tissue barriers: Drug delivery using cationic peptides and proteins. Nano Today 2020;34, 100898. 10.1016/j.nantod.2020.100898
13. Mehta S, Akhtar S, Porter RM, Önnerfjord P, Bajpayee AG. Interleukin-1 receptor antagonist (IL-1Ra) is more effective in suppressing cytokine-induced catabolism in cartilage-synovium co-culture than in cartilage monoculture. Arthritis Res Ther 2019;21:238. 10.1186/s13075-019-2003-y [PubMed: 31722745]
14. Chevalier X, Goupille P, Beaulieu AD, Burch FX, Bensen WG, Conrozier T, et al. Intraarticular injection of anakinra in osteoarthritis of the knee: A multicenter, randomized, double-blind, placebo-controlled study. Arthritis Rheum 2009;61:344–52. 10.1002/art.24096 [PubMed: 19248129]
15. Elsaid KA, Ubhe A, Shaman Z, D'Souza G. Intra-articular interleukin-1 receptor antagonist (IL1-ra) microspheres for post-traumatic osteoarthritis: in vitro biological activity and in vivo disease modifying effect. J Exp Orthop 2016;3:18. 10.1186/s40634-016-0054-4 [PubMed: 27539076]
16. Kraus VB, Birmingham J, Stabler TV, Feng S, Taylor DC, Moorman CT, et al. Effects of intraarticular IL1-Ra for acute anterior cruciate ligament knee injury: a randomized controlled pilot trial (NCT00332254). Osteoarthr Cartil 2012;20:271–8. 10.1016/j.joca.2011.12.009
17. Pelletier JP, Caron JP, Evans C, Robbins PD, Georgescu HI, Jovanovic D, et al. In vivo suppression of early experimental osteoarthritis by interleukin-1 receptor antagonist using gene therapy. Arthritis Rheum 1997;40:1012–9. 10.1002/art.1780400604 [PubMed: 9182910]
18. Caron JP, Fernandes JC, Martel-Pelletier J, Tardif G, Mineau F, Geng C, et al. Chondroprotective effect of intraarticular injections of interleukin-1 receptor antagonist in experimental osteoarthritis. Suppression of collagenase-1 expression. Arthritis Rheum 1996;39:1535–44. 10.1002/art.1780390914 [PubMed: 8814066]
19. Fernandes J, Tardif G, Martel-Pelletier J, Lascau-Coman V, Dupuis M, Moldovan F, et al. In vivo transfer of interleukin-1 receptor antagonist gene in osteoarthritic rabbit knee joints: prevention of osteoarthritis progression. Am J Pathol 1999;154:1159. 10.1016/S0002-9440(10)65368-0 [PubMed: 10233854]
20. Vedadghavami A, Wagner EK, Mehta S, He T, Zhang C, Bajpayee AG. Cartilage penetrating cationic peptide carriers for applications in drug delivery to avascular negatively charged tissues. Acta Biomater 2019;93:258–69. 10.1016/j.actbio.2018.12.004 [PubMed: 30529083]
21. He T, Zhang C, Colombani T, Bencherif SA, Porter RM, Bajpayee AG. Intra-articular kinetics of a cartilage targeting cationic PEGylated protein for applications in drug delivery. Osteoarthr Cartil 2023;31:187–98. 10.1016/j.joca.2022.09.010
22. Lotfy A, AboQuella NM, Wang H. Mesenchymal stromal/stem cell (MSC)-derived exosomes in clinical trials. Stem Cell Res Ther 2023;14:66. 10.1186/s13287-023-03287-7 [PubMed: 37024925]
23. Munagala R, Aqil F, Jeyabalan J, Gupta RC. Bovine milk-derived exosomes for drug delivery. Cancer Lett 2016;371:48–61. 10.1016/j.canlet.2015.10.020 [PubMed: 26604130]
24. Warren MR, Zhang C, Vedadghavami A, Bokvist K, Dhal PK, Bajpayee AG. Milk exosomes with enhanced mucus penetrability for oral delivery of siRNA. Biomater Sci 2021;9:4260–77. 10.1039/d0bm01497d [PubMed: 33367332]

25. Hajipour H, Farzadi L, Roshangar L, Latifi Z, Kahroba H, Shahnazi V, et al. A human chorionic gonadotropin (hCG) delivery platform using engineered uterine exosomes to improve endometrial receptivity. Life Sci 2021;275, 119351. 10.1016/j.lfs.2021.119351 [PubMed: 33737084]
26. Haney MJ, Klyachko NL, Zhao Y, Gupta R, Plotnikova EG, He Z, et al. Exosomes as drug delivery vehicles for Parkinson's disease therapy. J Control Release 2015;207:18–30. 10.1016/j.jconrel.2015.03.033 [PubMed: 25836593]
27. Cotto HAM, Pathrikar TV, Hakim B, Baby HM, Zhang H, Zhao P, et al. Cationic-motif-modified exosomes for mRNA delivery to retinal photoreceptors. J Mater Chem B 2024;12:7384–400. 10.1039/D4TB00849A [PubMed: 38946491]
28. Vedadghavami A, Mehta S, Bajpayee AG. Characterization of Intra-Cartilage Transport Properties of Cationic Peptide Carriers. J Vis Exp 2020. 10.3791/61340
29. Kondiboyina V, Boyer TL, Mooney N, Bajpayee AG, Shefelbine SJ. Effect of dynamic loading on calcium signaling in in-situ chondrocytes. J Biomech 2024;174, 112265.
30. Zhang C, He T, Vedadghavami A, Bajpayee AG. Avidin-biotin technology to synthesize multi-arm nano-construct for drug delivery. MethodsX 2020;7, 100882. 10.1016/j.mex.2020.100882
31. Kunze A, Bally M, Höök F, Larson G. Equilibrium-fluctuation-analysis of single liposome binding events reveals how cholesterol and Ca2+ modulate glycosphingolipid trans-interactions. Sci Rep 2013;3:1452. 10.1038/srep01452 [PubMed: 23486243]
32. Zhou Y, Lv M, Li T, Zhang T, Duncan R, Wang L, et al. Spontaneous calcium signaling of cartilage cells: from spatiotemporal features to biophysical modeling. FASEB J 2019;33:4675–87. 10.1096/fj.201801460R [PubMed: 30601690]
33. Gong X, Xie W, Wang B, Gu L, Wang F, Ren X, et al. Altered spontaneous calcium signaling of in situ chondrocytes in human osteoarthritic cartilage. Sci Rep 2017;7, 17093. 10.1038/s41598-017-17172-w [PubMed: 29213100]
34. Lv M, Zhou Y, Polson SW, Wan LQ, Wang M, Han L, et al. Identification of chondrocyte genes and signaling pathways in response to acute joint inflammation. Sci Rep 2019;9:93. 10.1038/s41598-018-36500-2 [PubMed: 30643177]
35. Selvadoss A, Baby HM, Zhang H, Bajpayee AG. Harnessing exosomes for advanced osteoarthritis therapy. Nanoscale 2024;16:19174–91. 10.1039/D4NR02792B [PubMed: 39323205]
36. Liu Q, Li D, Pan X, Liang Y. Targeted therapy using engineered extracellular vesicles: principles and strategies for membrane modification. J Nanobiotechnol 2023;21:334. 10.1186/s12951-023-02081-0
37. Zhang H, Yan W, Wang J, Xie S, Tao WA, Lee C-W, et al. Surface functionalization of exosomes for chondrocyte-targeted siRNA delivery and cartilage regeneration. J Control Release 2024;369:493–505. 10.1016/j.jconrel.2024.04.009 [PubMed: 38582335]
38. Ma S, Song L, Bai Y, Wang S, Wang J, Zhang H, et al. Improved intracellular delivery of exosomes by surface modification with fluorinated peptide dendrimers for promoting angiogenesis and migration of HUVECs. RSC Adv 2023;13:11269–77. 10.1039/d3ra00300k [PubMed: 37057265]
39. He T, Zhang C, Vedadghavami A, Mehta S, Clark HA, Porter RM, et al. Multi-arm Avidin nano-construct for intra-cartilage delivery of small molecule drugs. J Control Release 2020;318:109–23. 10.1016/j.jconrel.2019.12.020 [PubMed: 31843642]
40. De la Bajpayee Vega AG, Scheu RE, Varady M, Yannatos NH, Brown LAIA, et al. Sustained intra-cartilage delivery of low dose dexamethasone using a cationic carrier for treatment of post traumatic osteoarthritis. Eur Cell Mater 2017;34:341–64. 10.22203/eCM.v034a21 [PubMed: 29205258]
41. Tamrin SH, Phelps J, Nezhad AS, Sen A. Critical considerations in determining the surface charge of small extracellular vesicles. J Extracell Vesicles 2023;12, 12353. 10.1002/jev2.12353 [PubMed: 37632212]
42. Warren MR, Bajpayee AG. Modeling electrostatic charge shielding induced by cationic drug carriers in articular cartilage using donnan osmotic theory. Bioelectricity 2022;4:248–58. 10.1089/bioe.2021.0026 [PubMed: 36644714]
43. Warren MR, Vedadghavami A, Bhagavatula S, Bajpayee AG. Effects of polycationic drug carriers on the electromechanical and swelling properties of cartilage. Biophys J 2022;121:3542–61. 10.1016/j.bpj.2022.06.024 [PubMed: 35765244]

44. Zhang C, Vedadghavami A, He T, Charles JF, Bajpayee AG. Cationic carrier mediated delivery of anionic contrast agents in low doses enable enhanced computed tomography imaging of cartilage for early osteoarthritis diagnosis. ACS Nano 2023;17:6649–63. 10.1021/acsnano.2c12376 [PubMed: 36989423]
45. Feng K, Xie X, Yuan J, Gong L, Zhu Z, Zhang J, et al. Reversing the surface charge of MSC-derived small extracellular vesicles by εPL-PEG-DSPE for enhanced osteoarthritis treatment. J Extracell Vesicles 2021;10, e12160. 10.1002/jev2.12160
46. Jenei-Lanzl Z, Meurer A, Zaucke F. Interleukin-1β signaling in osteoarthritis – chondrocytes in focus. Cell Signal 2019;53:212–23. 10.1016/j.cellsig.2018.10.005 [PubMed: 30312659]
47. Irie K, Uchiyama E, Iwaso H. Intraarticular inflammatory cytokines in acute anterior cruciate ligament injured knee. Knee 2003;10:93–6. 10.1016/S0968-0160(02)00083-2 [PubMed: 12649034]
48. Anderson DD, Chubinskaya S, Guilak F, Martin JA, Oegema TR, Olson SA, et al. Post-traumatic osteoarthritis: Improved understanding and opportunities for early intervention. J Orthop Res 2011;29:802–9. 10.1002/jor.21359 [PubMed: 21520254]
49. Lorenzo P, Bayliss MT, Heinegård D. Altered patterns and synthesis of extracellular matrix macromolecules in early osteoarthritis. Matrix Biol 2004;23:381–91. 10.1016/j.matbio.2004.07.007 [PubMed: 15533759]
50. Bay-Jensen A-C, Hoegh-Madsen S, Dam E, Henriksen K, Sondergaard BC, Pastoureau P, et al. Which elements are involved in reversible and irreversible cartilage degradation in osteoarthritis? Rheumatol Int 2010;30:435–42. 10.1007/s00296-009-1183-1 [PubMed: 19816688]

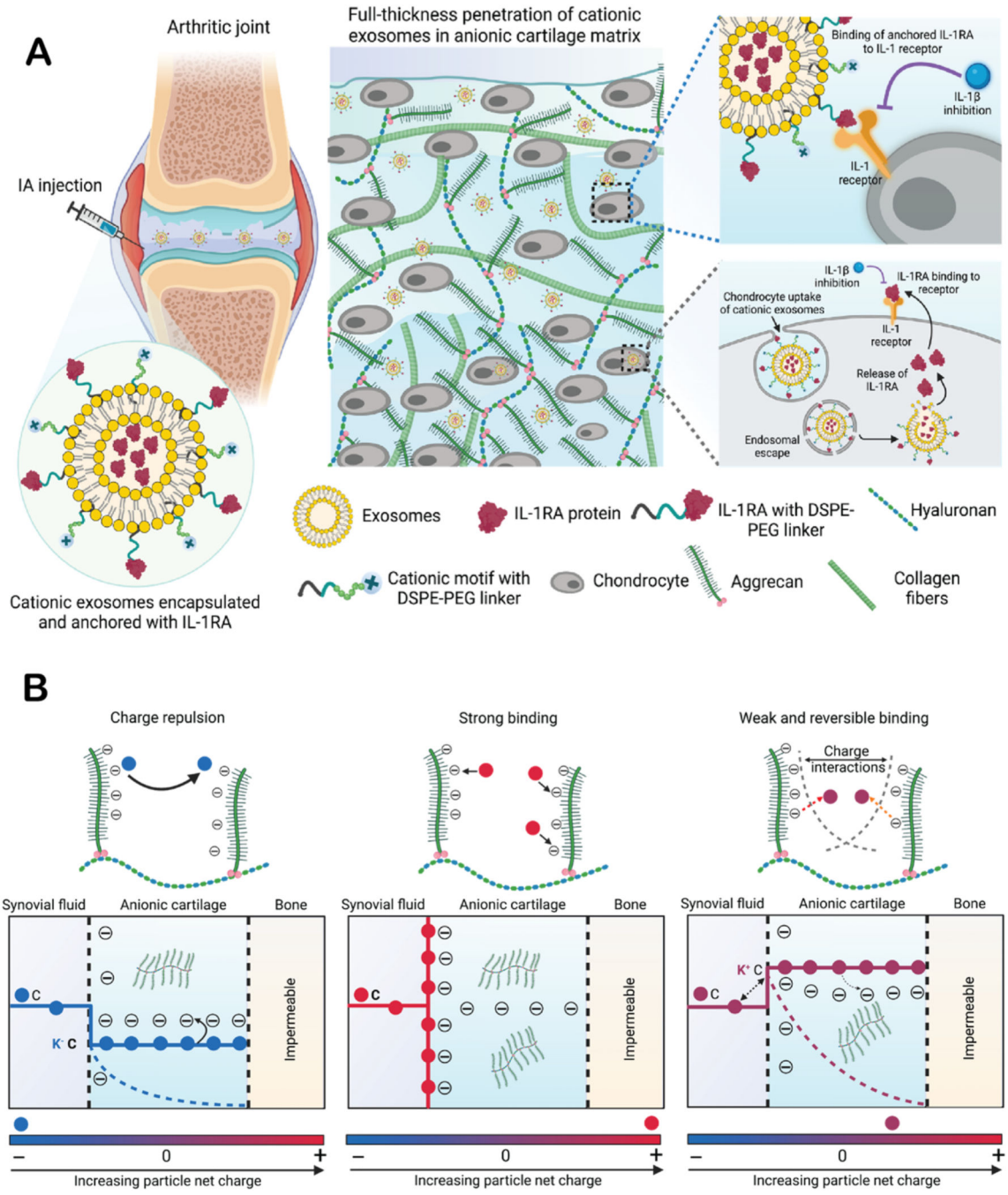

Fig. 1.

Concept of charge-based targeted drug delivery to cartilage. (A) Schematic representing the transport of IL-1RA-loaded cationic Exos through the cartilage tissue owing to electrostatic interactions. (B) Negatively charged carriers are electrostatically repelled by cartilage GAGs causing a downward partitioning of their concentration at the synovial fluid-cartilage interface from C to $K^{-}C$ that results in slower intra-tissue diffusion rates. However, excessive positive charge on carriers can result in their sticking within the cartilage superficial layer owing to strong binding interactions. Optimally charged cationic carriers

use weak reversible electrostatic binding interactions to penetrate through the full thickness of tissue resulting in a high intra-cartilage uptake. Their concentration partitions upward from C to K^+C facilitating faster transport rates.

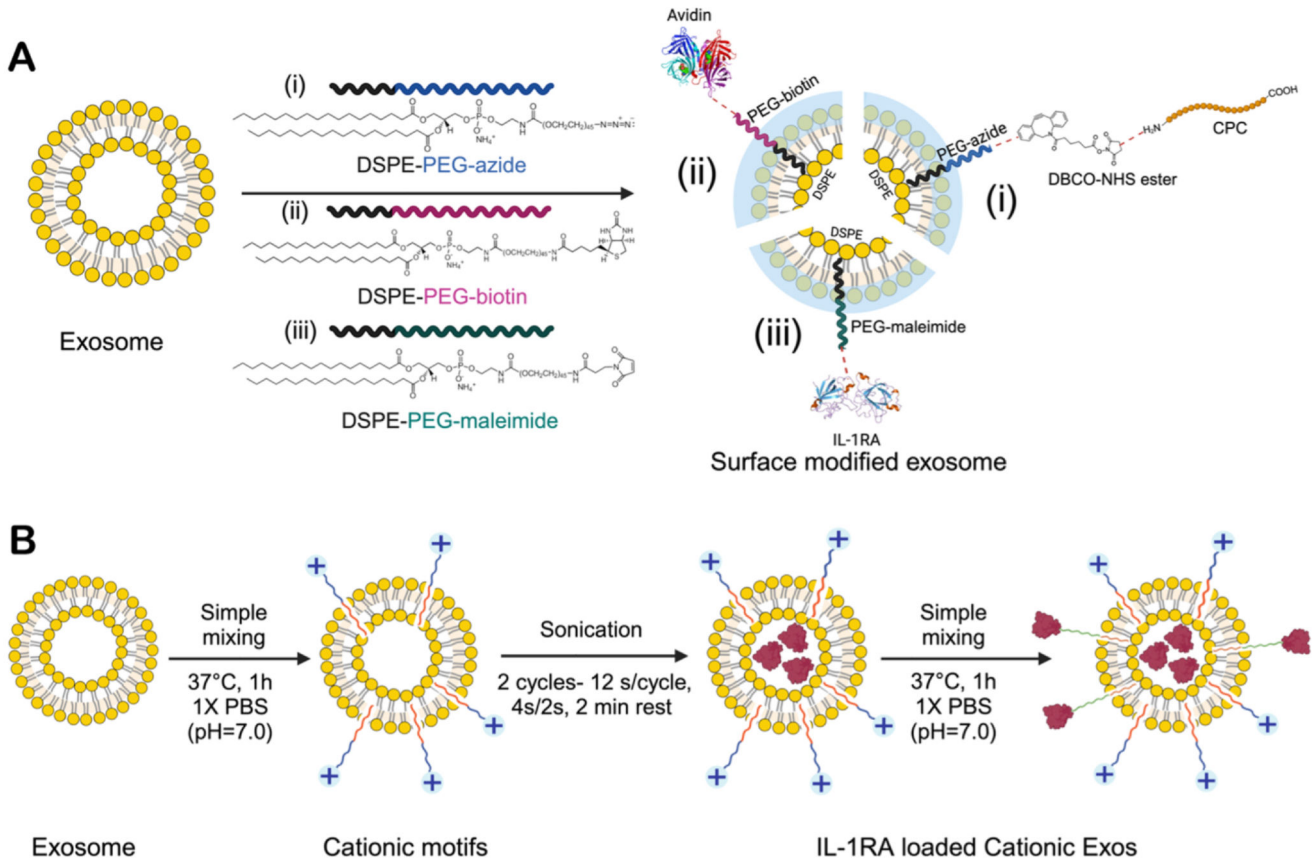

Fig. 2.

Schematics representing loading of cationic motifs and IL-1RA on Exos. (A) The surface of Exos is modified with cationic motifs and IL-1RA using various linkers: (i) DSPE-PEG-azide for CPC, (ii) DSPE-PEG-biotin for Av, (iii) DSPE-PEG-maleimide for IL-1RA, using copper-free click chemistry. (B) Incorporation of cationic motifs onto the Exo surface through a simple mixing process at 37 °C for 1 h in 1X PBS. Subsequently, IL-1RA is sonicated for 12 s per cycle (2 cycles) with a 4s/2s pulse, 2 min rest, and 20% amplitude. Finally, additional IL-1RA is introduced to the cationic Exos loaded with IL-1RA through a simple mixing step at 37 °C for 1 h in 1X PBS.

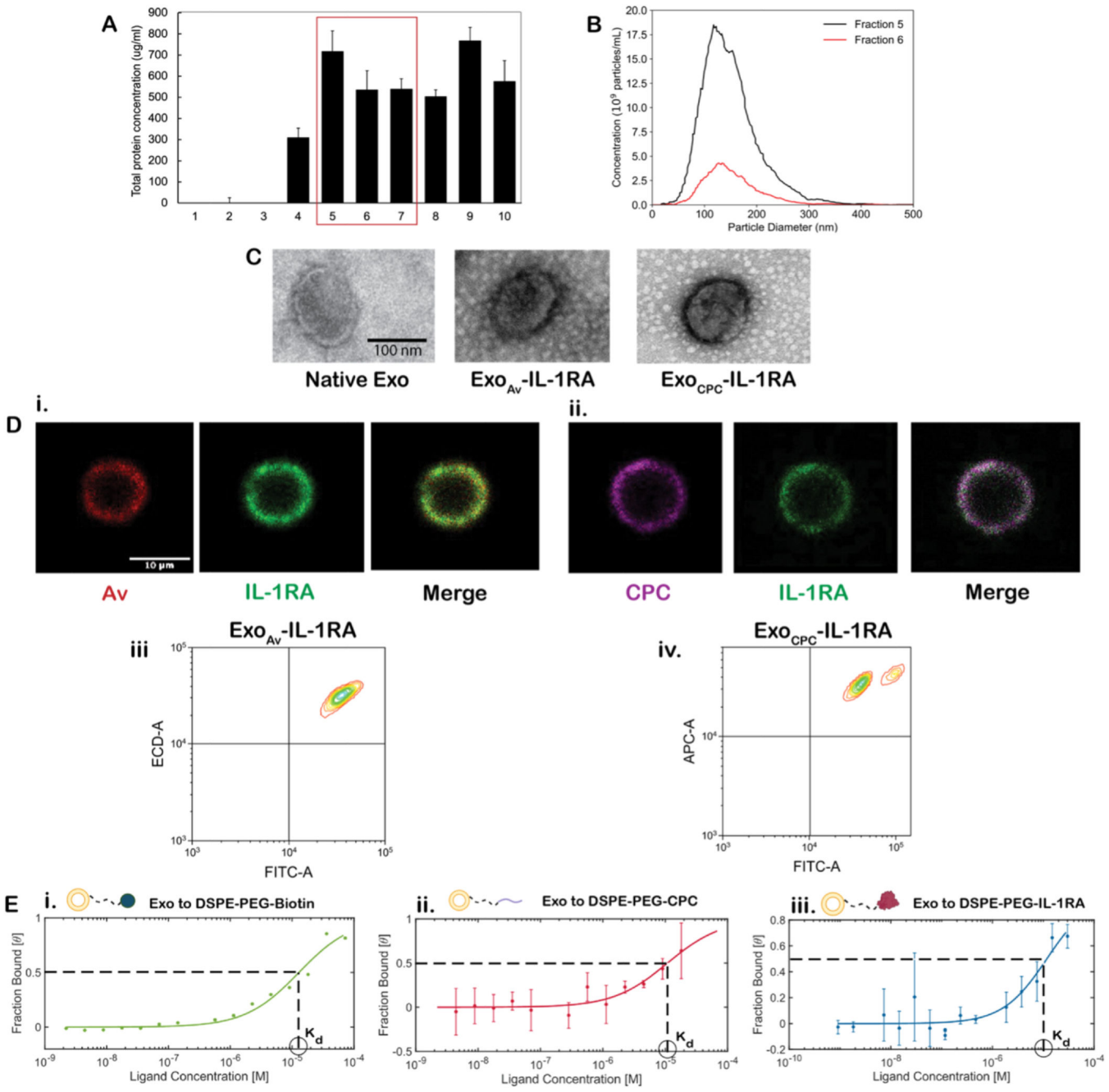

Fig. 3.

IL-1RA-loaded cationic Exos characterization. (A) Total protein content in SEC fractions after exosome harvest measured using BCA assay. Fractions 5, 6 and 7 indicate the highest protein content (red box). (B) The size of harvested exosomes was measured using NTA. (C) TEM images of Native Exos, Exo$_{Av}$-IL-1RA and Exo$_{CPC}$-IL-1RA. (D) Fluorescently labeled IL-1RA loaded cationic Exos anchored to CD63 antibody-coated magnetic beads for conjugation confirmation. Overlapped confocal images of (i) Av-Texas Red and IL-1RA-FITC for Exo$_{Av}$-IL-1RA and (ii) CPC-Cy5 and IL-1RA-FITC for Exo$_{CPC}$-IL-1RA, confirm the loading of cationic motifs and IL-1RA on the Exos. Flow cytometry data indicates

elevated (iii) Texas Red and FITC fluorescence for Exo_{Av}-IL-1RA and (iv) Cy5 and FITC fluorescence for Exo_{CPC}-IL-1RA. (E) Binding affinities of (i) DSPE-PEG-Biotin, (ii) DSPE-PEG-CPC and (iii) DSPE-PEG-IL-1RA to Exo compared using MST; respective K_d values are circled.

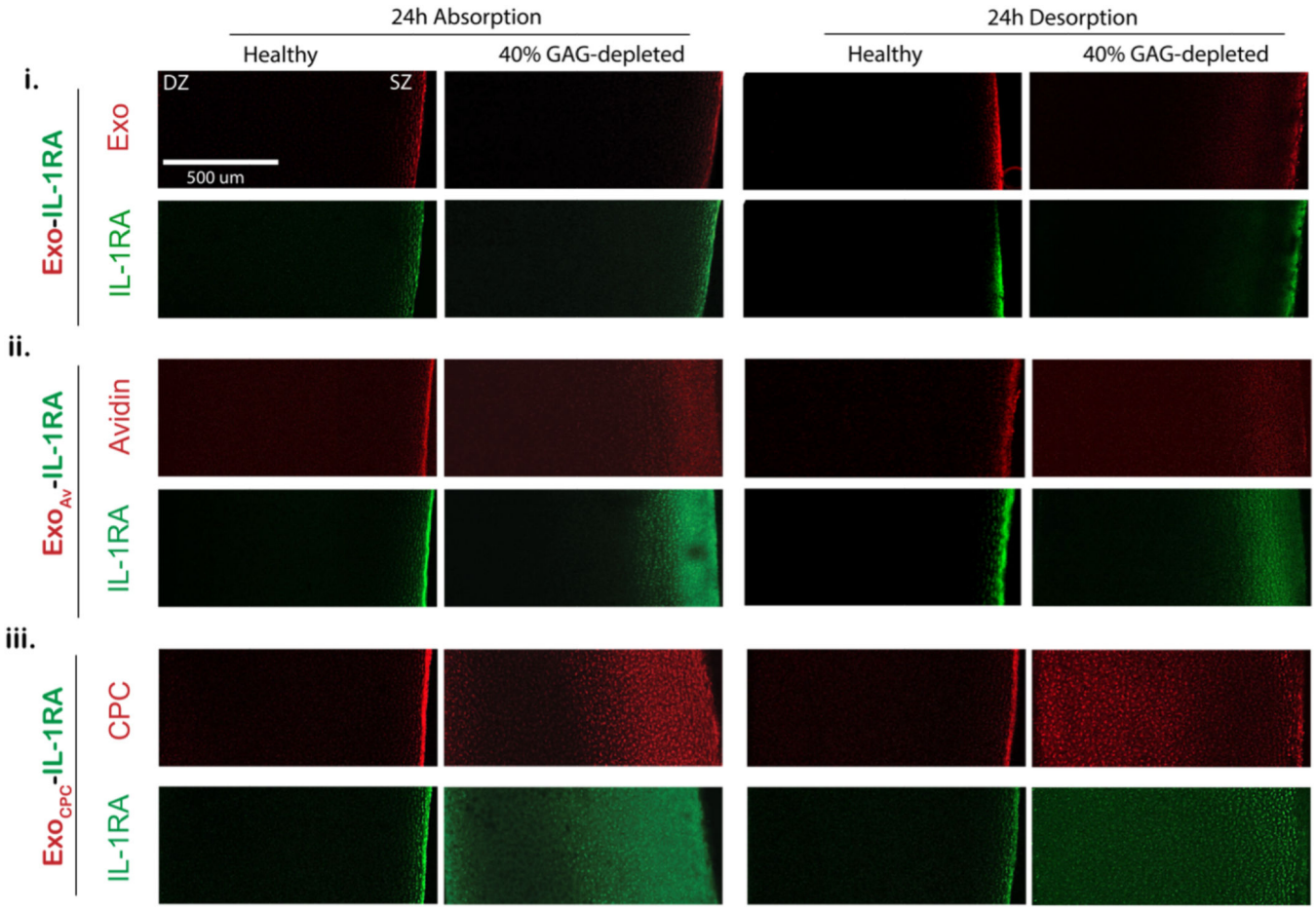

Fig. 4.

IL-1RA-loaded Cationic Exos transport and retention properties in cartilage. Confocal images representing 1D transport of (i) Exo-IL-1RA, (ii) Exo_{Av}-IL-1RA and (iii) Exo_{CPC}-IL-1RA in healthy and 40% GAG-depleted cartilage explants from SZ to DZ. Native Exo, Exo_{Av}, Exo_{CPC} are shown in red and IL-1RA is shown in green.

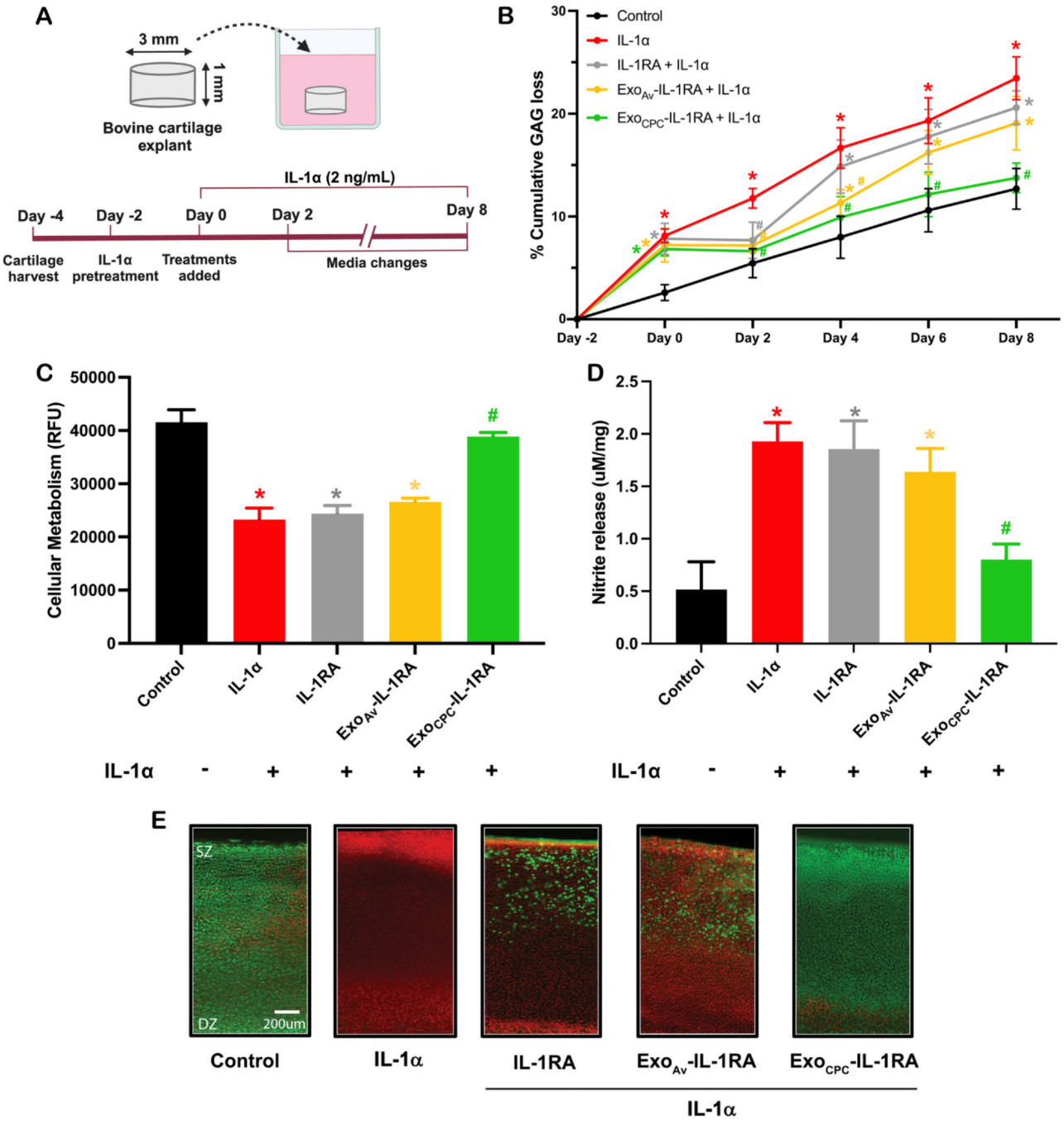

Fig. 5.

Effectiveness of a single dose of 5000 ng/mL free or cationic Exo-loaded IL-1RA in 2 ng/mL IL-1α treated bovine cartilage explants over 8 days. (A) Schematic of the experimental design, (B) % percent cumulative GAGs lost to media from cartilage explants over 8 days, (C) cellular metabolism and (D) nitrite release analyzed on day 8, (E) cartilage cell viability images taken on day 8; live and dead cells indicated by green and red. * vs control; # vs IL-1α $p < 0.05$.

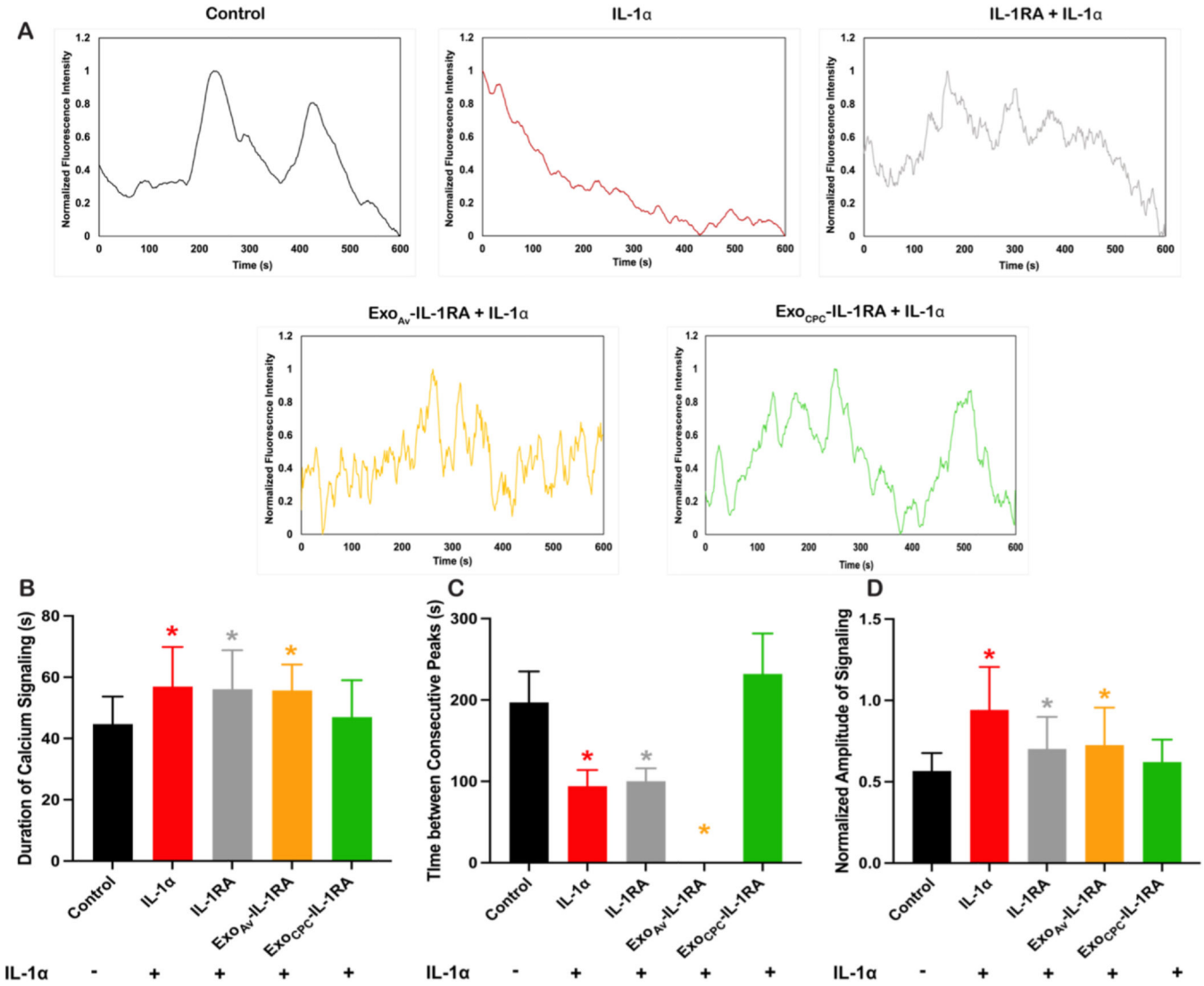

Fig. 6.

Effect of IL-1RA-loaded cationic Exos on chondrocytes. (A) Representative calcium signaling curves measured on day 8, (B-D) parameters of calcium signaling including duration of signaling, time between peaks and amplitude of signaling on day 8. * vs control; $p < 0.05$.

Table I

Cationic motif sequences, molecular weights (Da) and net charges.

Motif	Sequence	Molecular weight (Da)	Net charge
Avidin	-	66000	+6 ~ +20
CPC	$RRRR(NNRRR)_3R$	2889	+14

Table II

Loading of cationic motifs and IL-1RA on Exos, zeta potential (mV), size (nm) and PDI (%).

Exosomes	Loading (mol) / Exo (mol)		Zeta potential (mV)	Size (nm)	PDI (%)
	Cationic motif	IL-1RA			
Native Exo	-	-	−27.9 ± 3.0	197 ± 11	23.2 ± 0.4
Exo_{Av}-IL-1RA	217 ± 33	529 ± 26	−2.3 ± 0.8	213 ± 4	22.5 ± 1.6
Exo_{CPC}-IL-1RA	1102±29	495 ± 45	−1.6 ± 1.1	221 ± 7	14.6 ± 4.5

Table III

Mean binding affinities (Kd) ± confidence interval of DSPE-PEG-motifs to Exos assessed via initial fluorescence analysis using MST.

Target	Ligand	K_d± SD (μM)
Exo	DSPE-PEG-Biotin	12.9 ± 2.6
	DSPE-PEG-CPC	10.8 ± 8.2
	DSPE-PEG-IL-1RA	11.8 ± 6.4